AN INQUARY STUDY OF NiO FILMS DEPOSITED WITH SOL-GEL SPIN COATING

Guven Turgut

Erzurum Technical University, Erzurum/Turkey
guven.turgut@erzurum.edu.tr

Abstract: Y incorporated nickel oxide thin films have been deposited via sol-gel route by using spin coater. The structural, morphological and optical properties of films have been inquired. The films had nano-sized polycrystalline cubic structure. The optical characterizations indicated that the band gap and Urbach energy continuously went up with Y contribution. The present investigation reveals the properties of nickel oxide are healed and controlled with Y contribution and these films are probably good candidates for various applications.

Keywords: NiO, Sol-gel, Y doping

Introduction

Nickel oxide (NiO), which is one of transition metal oxides, is an intriguing material for magnetic and electrochromic applications, organic light emitting diodes, catalysts, smart windows and solar cells (Reguig et al., 2007; Turgut et al., 2015) antiferromagnetic feature, good optical transmittance with a wide band gap of 3.6-4.0 eV, thermal and chemical stableness (Patil et al., 2002; Gowthami et al., 2014). A stoichiometric NiO is a good insulator with resistivity of about 10^{13} ohm.cm**,** but non-stoichiometry, which is resulted from nickel vacancies and oxygen interstitials, makes it a p-type semiconductor material (Joshi et. al., 2006). The structural, magnetic, optical, electrical, morphological and electrochromic properties of NiO material can be improved by doping with foreign elements such as Li, Cu, K, P, Y and other elements. To the our the best knowledge, there is no report about investigation of Y doping effect on characteristic features of NiO. Therefore, it is necessary to make various studies in order to understand detailed influence of Y doping on properties of NiO. Hence, in present study, pure and Y doped NiO films have been fabricated via a sol-gel spin coating technique which is simple, safe, cheap and capable of fabricating homogenous and good quality films (Turgut et al., 2015) and Y doping effect on crystallographic, morphological and optical properties of NiO films have been investigated.

Material and Method

Pure (YNO-0), 1 at. % (YNO-1), 2 at. % (YNO-2), 3 at. % (YNO-3), 5 at. % (YNO-5) and 7 at. % (YNO-7) yttrium doped NiO thin films were prepared with spin coating by using nickel(II) acetate tetrahydrate, yttrium(III) chloride, methanol and monoethanolamine. After the solutions were prepared, they were aged for three months and finally solutions were dribbled onto micro slide glasses that were spun at velocity of 3500 rpm for 25 seconds by spin coater. The pre-grown layers were sintered at 200 ^{o}C for 10 min. This procedure was reiterated for ten times. Lastly, the whole samples were annealed at 550 ^{o}C for 1 hour in air. The crystallographic, surface and optical features of pure and Y doped films were inquired by a Rigaku/Smart Lab x-ray diffractometer (XRD), Nanomagnetic Instruments AFM (atomic force microscope), Perkin Elmer UV/VIS Lambda 35 spectrophotometer.

Results and Discussions

The XRD patterns in Fig.1 reveal all films have polycrystalline cubic bunsenite NiO structure (JCPDS card no: 47–1049) with (200) preferential orientation.

Sta et al. (2014) observed the similar crystallographic structure for Li doped NiO films prepared by sol-gel spin coating. As seen from Fig.1, the peaks' intensities gradually decrease with Y contribution, which suggests Y doping causes a deteriorating in the crystallinity of NiO. The textured coefficient (TC) is calculated by Eq. (1)

$$TC_{(hkl)} = \frac{I_{(hkl)}/I_0}{(\frac{1}{N})\sum I_{(hkl)}/I_0} \quad (1)$$

where I_{hkl}, $I_{0(hkl)}$ and N are the intensities of relative and standard peak, the number of peaks.

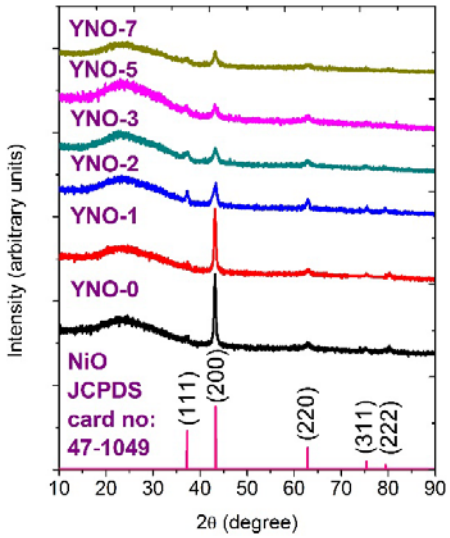

Figure 1. The XRD patterns of YNO thin films

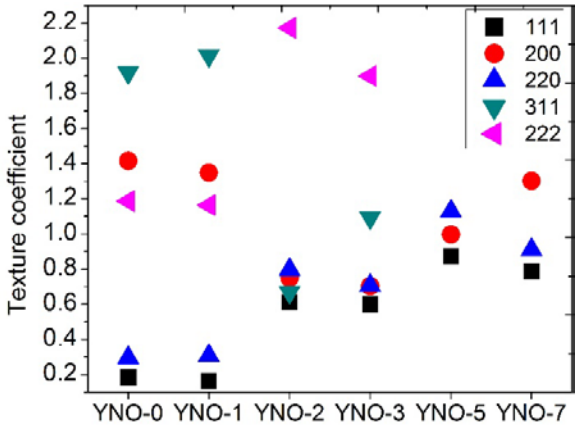

Figure 2. The variation of TC values of NiO with Y doping

The alteration of TC values with Y doping (Fig. 2) indicates that the TC values of some peaks are greater than one and this remarks the more crystallites than one are directed at those orientations (Duman et al., 2014). The mean crystallite size (D) and micro-strain values for samples are identified by Eqs. (2) and (3)

$$D = \frac{0.9\lambda}{(\beta cos\theta)} \quad (2)$$

$$\varepsilon = \left(\frac{1}{sin\theta}\right)\left[\left(\frac{\lambda}{D}\right) - (\beta cos\theta)\right] \quad (3)$$

where β is full width at half of the peak maximum (FWHM) and it is computed by $\beta^2 = \beta^2_{obs} - \beta^2_{inst}$ (β_{obs} is measured from XRD, β_{inst} is instrumental broadening). The mean crystallite size value for undoped sample continuously decreases from 21.32 nm to 20.80 nm, 17.77 nm, 17.06 nm, 15.76 nm and 13.84 nm for YNO-1, NYO-2, NYO-3, NYO-5 and NYO-7 samples. However, the micro-strain value gradually increases from $1.96x10^{-3}$, to the values of $2.01x10^{-3}$, $2.35x10^{-3}$, $2.64x10^{-3}$, $2.98x10^{-3}$ and $3.04x10^{-3}$ with Y doping. These results clearly indicate that the crystallinity of films decreases with Y doping ratio. The decreasing crystallinity of NiO with Y doping can be resulted from higher ionic radius of Y^{3+} (0.90 Å) than Ni^{2+} (0.69 Å) (Greenwood and Earnshaw, 1997). The difference between ionic radii can introduce a lattice distortion and an increase in amount of disorders.

The 2D and 3D AFM micrographs (Fig. 3) show there are nano-sized particles on the surfaces of films and their distribution is nearly homogenous. These images also exhibit the particle size incessantly decreases with raising Y doping ratio. This alteration is very good consistent with variation of crystallite size determined from XRD analysis. The surface roughness value of NiO film initially decreases from 1.23 nm to 0.98 nm, 0.94 nm and 0.62 nm with Y doping up to 3 at. % content and then it starts to increase to the values of 0.96 nm and 1.05 nm with more Y doping.

.

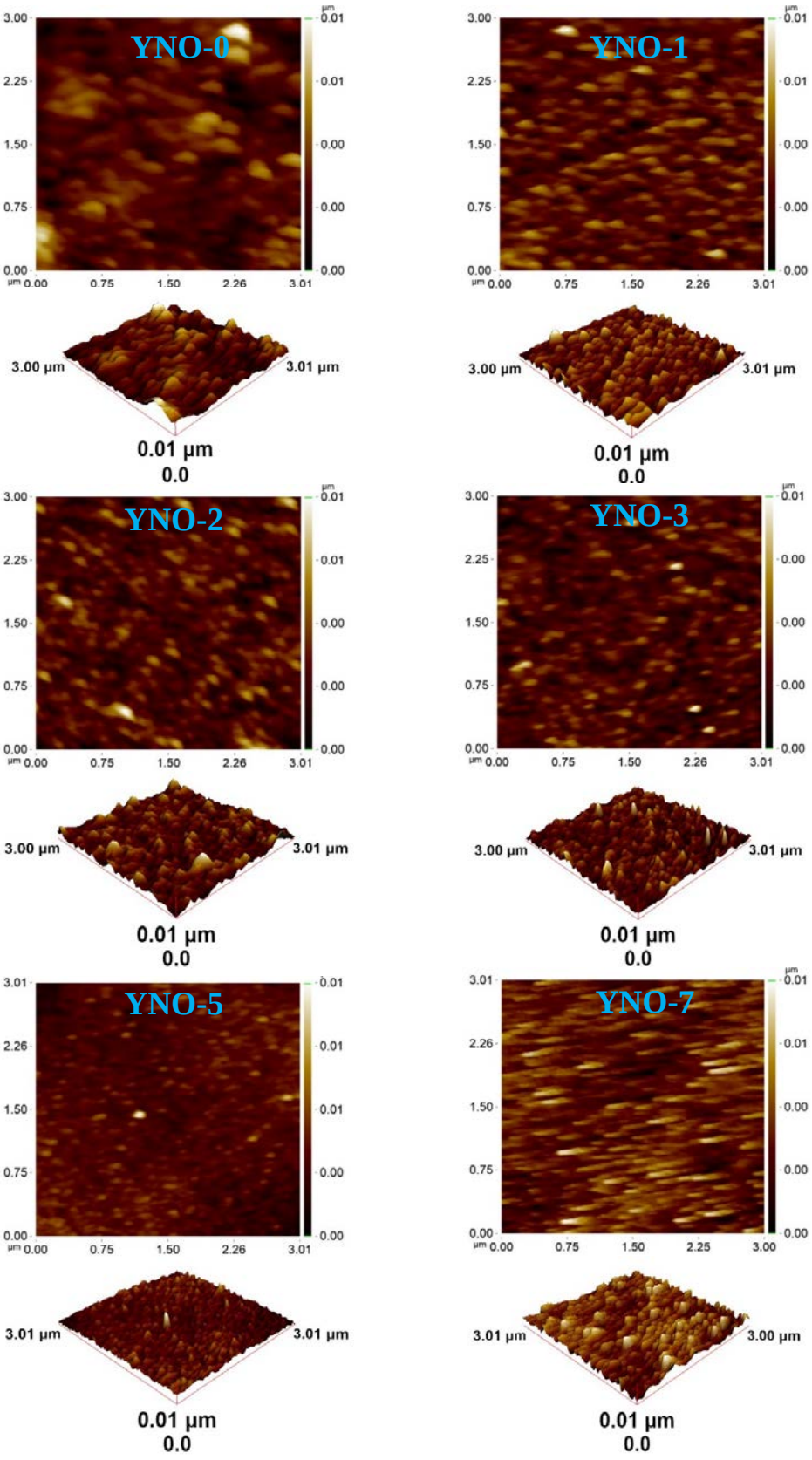

Figure 3. The AFM images of YNO thin films

The transmittance and $(\alpha h\nu)^2$ vs. $h\nu$ graphs are given in Fig. 4a-b. The transmittance values are about 80 %-96 % over wavelength range of 450-1100 nm. The value of optical band gap (E_g) is calculated by Eqs. (4), (5)

$$\alpha = \ln(1/T)/d \quad (4)$$

$$\alpha h\nu = K(h\nu - E_g)^{1/2} \quad (5)$$

where α, T, d and K are absorption coefficient, transmittance, film thickness and constant. As seen from $(\alpha h\nu)^2$ vs. $h\nu$ graphs (Fig. 4b), the E_g value for pure NiO film continuously increases from 3.274 eV to 3.809 eV with Y doping. An increasing in E_g with Y doping is probably resulted from decreasing crystallite size, which is clearly seen from XRD and AFM analysis

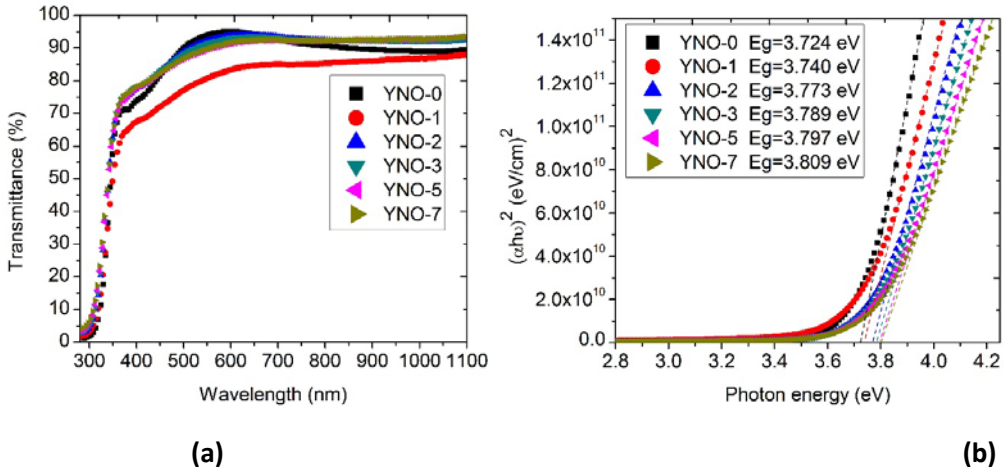

Figure 4. (a) The optical transmittance (b) $(\alpha h\nu)^2$ vs. (hν) curves of YNO films

This is known to be quantum confinement effect and band gap of a semiconductor is reversely proportional to crystallite size (Lin et al., 2005). The similar result was also observed for P doped NiO films (Das et al., 2010). The absorption tail is also inquired for deposited films. The absorption edge is called as the Urbach tail (Urbach, 1953) and it is given by Eq. (6)

$$\alpha(E,T) = \alpha_0 \exp\left(\frac{E-E_0}{E_u(T,X)}\right) \quad (6)$$

The Urbach energy (E_u) is related to temperature (T) and crystal disorders (X). However, Cody et al. (1981) indicated non-thermal component depending on the structural disorders. Hereby, E_u values are determined by Eq. (7)

$$\ln\alpha = E\frac{1}{E_u}\cdot\left(\ln(\alpha_0) + \frac{E_0}{E_u}\right) \quad (7)$$

$E_u = \Delta(h\nu)/\Delta(\ln\alpha)$ and it is based only on the degree of structural disorders. From Fig.5, the Urbach energy value of pure NiO gradually increases with increasing Y doping ratio.

This suggests Y incorporation into NiO causes a significant raise in the E_u values as a result of increasing structural disorders, which is seen from XRD analysis. An interesting point for this study is that E_g and E_u have a similar variation with Y doping ratio. The transitions from tail and band to tail because of expanding of Urbach tail would cause a decrease in E_g. But as indicated before, decreasing crystallite size is dominant factor for increasing optical band gap. A similar tendency between E_g and E_u was found for ZnO semiconductor material (Demirselcuk and Bilgin, 2013).

Conclusion

In this investigation, Y doped NiO samples were synthesized for the first time by sol-gel spin coating. The crystallographic and topographic investigations showed the samples were made of nano-sized particles with bunsenite NiO structure. The crystallinity and crystallite size decreased with Y content, however the values of micro-strain, optical band gap and Urbach energy increased with Y contribution level. It can be concluded the features of NiO films may be altered with Y doping.

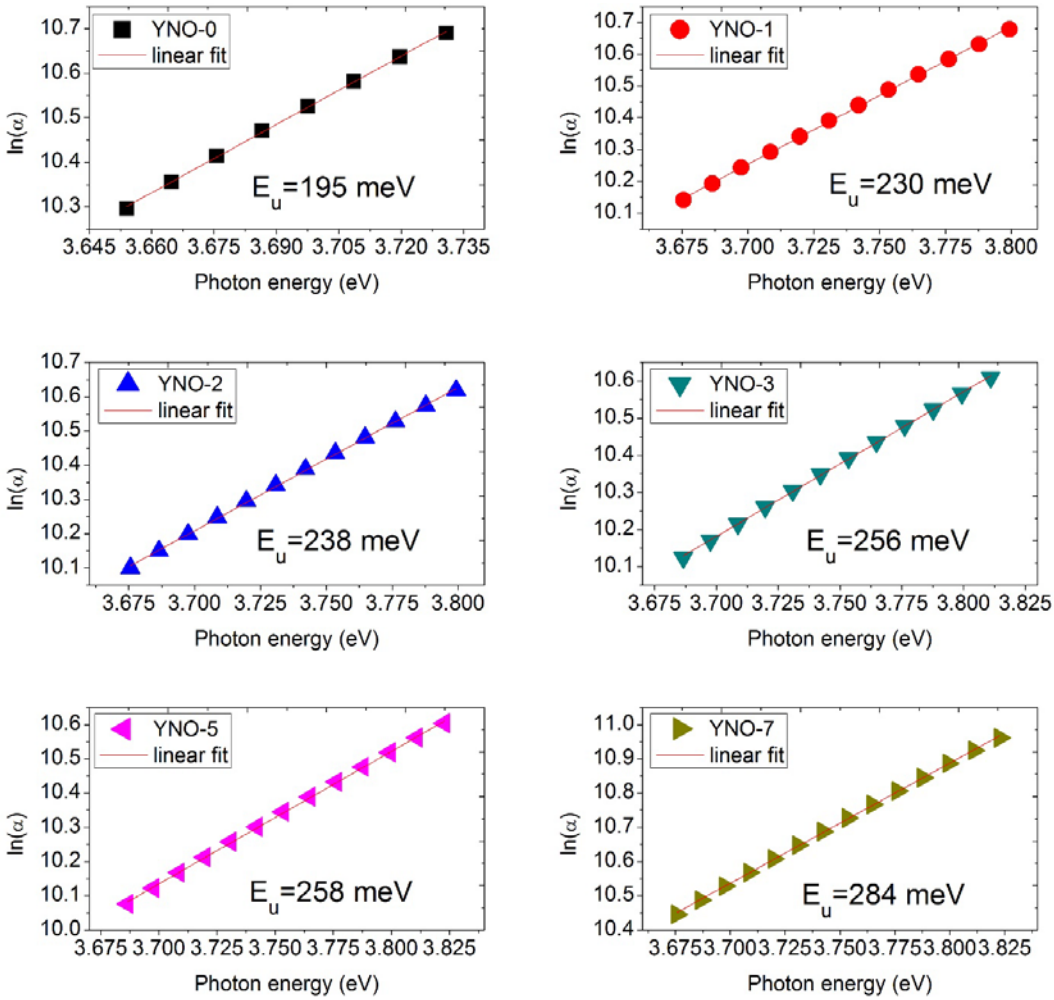

Figure 5. The curves of lnα vs. photon energy

References

Cody, G.D., Tiedje, T., Abeles, B., Brooks, B., Goldstein, Y. (1981). *Disorder and the Optical-Absorption Edge of Hydrogenated Amorphous Silicon*. Physics Review Letters vol. 47 pp. 1480-1483.

Das, N.S., Saha, B., Thapa, R., Das, G.C., Chattopadhyay, K.K. (2010). *Band gap widening of nanocrystalline nickel oxide thin films via phosphorus doping*. Physica E vol. 42 pp. 1377-1382.

Demirselcuk, B. and Bilgin, V. (2013). *Ultrasonically sprayed ZnO:Co thin films: Growth and characterization.* Applied Surface Science vol. 273 pp.478-483.

Duman, S., Turgut, G., Özçelik, F.Ş., Gürbulak, B. (2014). *The synthesis and characterization of sol–gel spin coated CdO thin films: As a function of solution molarity*. Materials Letters vol. 126 pp. 232-235.

Gowthami, V., Perumal, P., Sivakumar, R., Sanjeeviraja, C. (2014). *Structural and optical studies on nickel oxide thin film prepared by nebulizer spray technique.* Physica B vol. 452 pp.1-6.

Greenwood, N.N., Earnshaw, A. (1997). *Chemistry of the Elements.* 2nd ed. Oxford: Reed Edu Prof Publishing.

Joshi, U.S., Matsumoto, I., Itaka, K., Sumiya, M., Koinuma, H. (2006). *Combinatorial synthesis of Li-doped NiO thin films and their transparent conducting properties.* Applied Surface Science vol. 252 pp. 2524-2528.

Lin, K.-F., Cheng, H.-M., Hsu, H.-C., Lin, L.-J., Hsien, W.-F. (2005). *Band gap variation of size-controlled ZnO quantum dots synthesized by sol–gel method*. Chemical Physics Letters vol. 409 pp. 208-211.

Patil, P.S., Kadam, L.D. (2002). *Preparation and characterization of spray pyrolyzed nickel oxide (NiO) thin films.* Applied Surface Science vol. 199 pp. 211-221.

Reguig, B.A., Khelil, A., Cattin, L., Morsli, M., Bernède, J.C. (2007). *Properties of NiO thin films deposited by intermittent spray pyrolysis process.* Applied Surface Science vol. 253 pp. 4330-4334.

Sta, I., Jlassi, M., Hajji, M., Ezzaouia, H. (2014). *Structural, optical and electrical properties of undoped and Li-doped NiO thin films prepared by sol–gel spin coating method.* Thin Solid Films vol. 555 pp.131-137.

Turgut, G., Sonmez, E., Duman, S. (2005) *Determination of certain sol-gel growth parameters of nickel oxide films.* Ceramics International vol. 41 pp. 2976-2989.

Urbach, F. (1953). *The Long-Wavelength Edge of Photographic Sensitivity and of the Electronic Absorption of Solids.* Physics Review vol. 92 pp.1324.